CONSEQUENCE ASSESSMENT OF THE BBC HYDROGEN REFUELING STATION, USING THE ADREA-HF CODE

E. Papanikolaou[1, 3], A.G. Venetsanos[1], M. Schiavetti[2], A. Marangon[2], M. Carcassi[2], N. Markatos[3]

[1] Environmental Research Laboratory, National Centre for Scientific Research Demokritos, 15310, Aghia Paraskevi Attikis, Greece
venets@ipta.demokritos.gr
[2] Università degli Studi di Pisa, Dipartimento di Ingegneria Meccanica Nucleare e della Produzione, via Diotisalvi 2, 56126, Pisa, Italy
[3] National Technical University of Athens, School of Chemical Engineering, Department of Process Analysis and Plant Design, Heroon Polytechniou 9, 15780, Zografou, Greece

ABSTRACT

Within the framework of the internal project HyQRA of the HYSAFE NoE, funded by EC, the participating partners were requested to apply their quantitative risk assessment (QRA) methodologies on an agreed predefined hypothetical gaseous hydrogen fueling station, the BBC station (Benchmark Base Case). The overall aim of the HyQRA was to perform an inter-comparison of the various QRA approaches and identify any knowledge gaps on data and information used in the QRA steps specifically related to hydrogen. Within this internal project, partners NCSRD and UNIPI collaborated on a common QRA. UNIPI identified the hazards on site, selected the most critical ones, defined the events that could be the primary cause of an accident and provided to NCSRD the scenarios listed in risk order for the evaluation of the consequences. NCSRD performed the quantitative analysis using the ADREA-HF CFD code. The predicted spatial and transient evolution of the formed flammable hydrogen-air clouds in the realistic geometry were provided to UNIPI for analysis of the consequences and evaluation of the risk and distances of damage to suggest improvements in the design and management of the BBC station to reduce the risk. In total fifteen scenarios were simulated. The first five were hydrogen releases in confined ventilated environment. Three scenarios concerned leaks inside the compression building, a small leak, a large leak and a pipeline rupture (initial flow rates 0.0114 kg/s, 0.0456 kg/s and 1.14 kg/s respectively), under 150 ACH mechanical ventilation conditions. Two scenarios concerned leaks inside the purification/drying building, a small leak and a pipeline rupture (initial flow rates 0.000138 kg/s and 0.0312 kg/s), under 150 ACH mechanical ventilation as well. The remaining ten scenarios were releases in open/semi-confined environment. Four scenarios concerned the storage cabinet, a small leak and a pipeline rupture (initial flow rates 0.0118 kg/s and 1.18 kg/s), under two ambient wind speed conditions (1.5 and 5 m/s). Four scenarios concerned the storage bank, a leak from one cylinder and a leak fed from the storage bank (0.0472 kg/s initial flow rates in both cases), at two wind speed conditions as above. Finally, the last two scenarios concern a large leak (0.0472 kg/s initial flow rate) from the refueling hose of one dispenser, at two wind speed conditions, as above. This paper presents the CFD methodology applied and discusses the results obtained from the performed calculations.

1 INTRODUCTION

Research into hydrogen energy and technology applications is part of the overall efforts to address the challenges of climate change, air pollution and energy independence. Specifically, the hydrogen fuel vehicles are considered to offer many benefits such as zero emissions and improved overall efficiency. Going one step further, the supporting fueling infrastructure is an essential component to the successful adoption of future hydrogen vehicles. Currently, 173 hydrogen fueling stations exist worldwide [1]. Most of them were built for demonstration and testing purposes whereas a few are open to the public. 58 stations are planned to be built in the near future [1]. However, before hydrogen fueling stations become a commonplace in the market, issues such as storage technology, containment, delivery and most of all safety requirements need to be addressed.

Concerning the safety issues of hydrogen fueling stations the establishment of a risk assessment methodology and associated data is essential to performing risk evaluations for demonstrating that a fueling station meets certain safety requirements. On the other hand, risk-informed permitting processes already exist in some countries and are being developed in other [2]. Clearly, there is a rising need to identify risk criteria, Quantitative Risk Assessment (QRA) techniques and data related to hydrogen fueling stations.

Chitose K. et al. [3] presented a framework for the methodology of a quantitative risk analysis and risk assessment guidance system for a small scale demonstration H2 fueling station. Probabilistic risk analysis for a nuclear plant was used as a reference for the quantitative risk assessment, HAZOP (HAzard and OPerability Studies) was applied for the identification of the hazards and the probability of the occurrence of an event and component failure rates were obtained from chemical plant data. Nilsen, S. et al. [4] presented a method for the determination of hazardous zones for a generic gas hydrogen fueling station based on the Italian Method. The work included a) sensitivity studies to examine the effect of equipment failure frequencies, leak sizes and environmental conditions on the type and extent of hazardous zones and b) quantitative estimations on the effect of ventilation and release location on the size of flammable cloud with the use of CFD and simpler numerical tools. The use of hydrogen concentration limits as a basis to define the extent of the hazardous zones was also discussed. LaChance, J. et al. [2] described in their paper an approach for risk-informing the permitting process for hydrogen fueling stations that relies primarily on the establishment of risk-informed codes and standards. The paper of Haugom, G.P., et. al. [5] described the work undertaken to determine the risk exposure of 3rd parties based on risk assessment studies for a planned hydrogen demonstration facility consisting of H2 production, storage, heat and power production and filling units. LaChance, J. [6] presented an application of QRA methods focusing on the minimum separation distances of a hydrogen refueling station code requirements. Experimentation and modeling work was included to serve as an input for assessing different release scenarios and into QRA. The QRA method was applied to the storage area of a medium size hydrogen fueling facility at 70MPa. The author stated that supporting data related to hydrogen to quantify the event tree and the phenomenological event probabilities were difficult to obtain. The important parameters for selecting separation distances were the selected consequence measures and risk criteria, the operating parameters and the availability of mitigation features. Finally, the author concluded that the results were sensitive to key modeling assumptions and the component leakage rates used in the QRA. Kikukawa, S. et al. [7] presented a risk assessment approach for liquid hydrogen fueling station of 17.000 lt storage capacity. FMEA (Failure Mode and Effect Analysis) and HAZOP methods were used for the identification of accident scenarios whereas the consequence level for each scenario was evaluated from data from liquid hydrogen explosion experiments. Finally, in the papers of Middha et al. [8] and Venetsanos et al. [9], the importance of using a validated for hydrogen CFD code as a tool in the procedure of risk assessment of hydrogen applications is highlighted. CFD codes can take into account the effects of buildings, the arrangement of different units and mitigation measures in contrast to the simplified tools and techniques.

The main objective of this work is the presentation of the quantitative analysis performed by NCSRD within the internal project HyQRA of the HYSAFE NoE [10], co-funded by EC. The overall aim of HyQRA was to perform an inter-comparison of the various QRA approaches applied by the participating partners on an agreed predefined hypothetical gaseous hydrogen fueling station, the BBC station (Benchmark Base Case) and identify any knowledge gaps on data and information used in the QRA steps specifically related to hydrogen. Within this internal project, NCSRD and UNIPI partners collaborated on a common QRA. UNIPI identified the hazards on site, selected the most critical ones, defined the events that could be the primary cause of an accident and provided to NCSRD the scenarios listed in risk order. NCSRD performed the quantitative analysis using the integral code GAJET and the ADREA-HF CFD code. The predicted spatial and transient evolution of the formed flammable hydrogen-air clouds in the realistic geometry were provided to UNIPI. UNIPI also performed a quantitative analysis of some of the open/semi-confined scenarios using the numerical code Effects 7.6 [11]. The results of the two different approaches were compared. UNIPI evaluated the consequences as a function of overpressure and heat radiation to determine the distances of damage.

2 DESCRIPTION OF THE BBC HYDROGEN REFUELING STATION

A gaseous hydrogen fueling station was used as a Benchmark Base Case (BBC) for the QRA exercise. The proposed BBC station layout was limited to the most essential units (purification/drying and compression buildings, storage bank, storage cabinet and 3 dispensers) as the aim of the exercise was to evaluate the different QRA methodologies, highlight the differences and identify the knowledge gaps and not to present an exhaustive risk assessment of a detailed fueling station layout. The surroundings of the station were a school, a restaurant, apartments, a shopping mall and offices. The rest of the objects were trees. Figure 1 shows the layout of the BBC station and its surroundings. The information of the BBC station geometry and specifications was taken from [12] and [13].

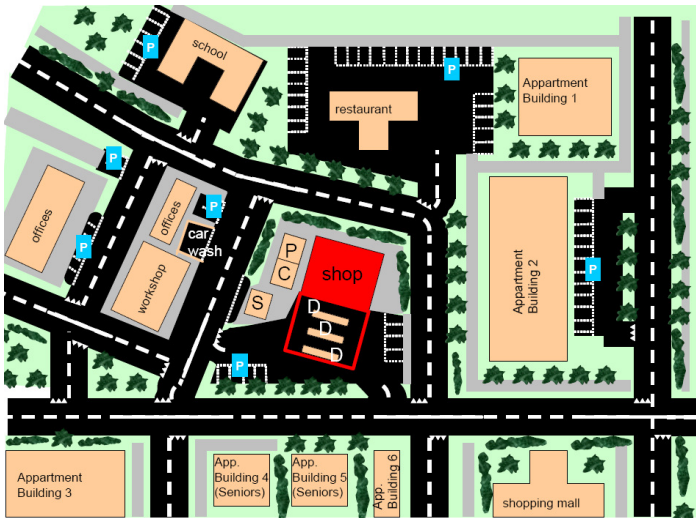

Figure 1: Layout of the BBC station and its surroundings (taken from [12])

3 QUANTITATIVE RISK ANALYSIS (QRA)

The Quantitative Risk Analysis of the BBC station by UNIPI consisted of the following steps:

a) Identification of the hazards: analysis of all equipment on site and their functions, identification of all possible deviations, causes and consequences (using the indexes for likelihood (L), severity (S) and risk (R), where $(R) = (L) \cdot (S)$). The likelihood indexes were obtain from literature whereas the severity indexes were determined on a qualitative judgment for open and confined environments.

b) Selection of the most critical events/hazards: the selection was done through the "Fundamental Risk Matrix" which categorized the events into Non Acceptable Risks (red region), Almost Acceptable Risks or ALARP -As Low As Reasonably Possible- (yellow region) and Acceptable Risks (white region), based on the (R) index. At this stage, no reference of the information of the emergency/detection systems present on site was used.

The first two steps were based on the HAZID (HAZard IDentification) methodology

c) Definition of the events that are the primary cause of an accident ("initiating" events): A revision of events located in the red and yellow zones of the "Fundamental Risk Matrix" was done taking into account the emergency/detection systems. The availability of the emergency/detection systems were evaluated through a quantitative fault tree analysis using the frequencies of the failures of H2 detection systems, the differential pressure-temperature transducers and the emergency shut down systems. A re-evaluation of the frequency of occurrence of an accidental

sequence was done through a quantitative event tree analysis using information from the literature. A "Compensated Risk Matrix" was formed. The scenarios that were still located in the red and yellow zones were selected for a quantitative evaluation of the consequences.

d) Evaluation of the consequences and estimation of vulnerabilities: A list of the proposed scenarios for consequence evaluation was prepared by UNIPI. NCSRD calculated the dispersion for all scenarios using the CFD code ADREA-HF. The dispersion of some of the open/semi-confined scenarios was also calculated by UNIPI using the numerical code Effects 7.6. For the open/semi-confined scenarios UNIPI calculated the overpressure (300, 100, 30 and 10 mbar) distances with the MEM method using as input both the dispersion results provided by NCSRD and the results of Effects 7.6 and performed an inter-comparison. The Effects 7.6 results were also used with the Chamberlain model to estimate the thermal radiation (35, 10 and 3 kW/m^2) distances. UNIPI prepared contour plots of explosion overpressures and thermal radiation in the BBC layout.

4 CONSEQUENCE ASSESSMENT USING THE INTEGRAL CODE GAJET AND THE ADREA-HF CFD CODE

As mentioned above, partner UNIPI prepared a set of 15 scenarios to be simulated, covering confined (compression and purification buildings) and open/semi-confined geometries (storage cabinet, storage bank and dispensers) [14]. NCSRD simulated all scenarios. The integral code GAJET [15] was used for the release calculations whereas the CFD dispersion Code ADREA-HF [16] was used for the dispersion calculations. Validation of the GAJET integral code can be found in [17].An overview of the validation of the ADREA-HF code for hydrogen applications can be found in [9]. For all simulations reported herein turbulence was modeled using the standard k-epsilon model [18], [19] extended for buoyant flows [20], [21]. A value of 0.72 was used for the turbulent Schmidt number.

4.1 Confined scenarios

Three scenarios concerning the compression building were described in the UNIPI report [14], a small leak (C1), a large leak (C2) and a pipeline rupture (C3). For the purification building, a small leak (P1) and a pipeline rupture (P2) was described. The dimensions of each building were 3m, 7m and 3.01m in X, Y and Z direction respectively. The ventilation of both buildings was provided by two means, the louvers on the two side walls and the fan in the middle of the ceiling providing 150 ACH (Air Changes per Hour).

Table 1: Description of confined scenarios

Scenario	Diameter of leak (m)	Leak direction	H2 inventory (m^3)	Temperature (K) and pressure (bar) in the cooler
C1	0.0008	downwards	0.25	313.15, 451
C2	0.0016	downwards	0.25	313.15, 451
C3	0.008	horizontal	0.25	313.15, 451
P1	0.0008	downwards	0.5	293.15, 5
P2	0.012	horizontal	0.5	293.15, 5

4.1.1 Release and dispersion calculations

For the release calculations the integral code GAJET was used assuming isentropic change and sonic flow with discharge coefficient 0.8. The temporal variation of temperature, pressure, density and velocity were calculated as exit conditions. The results from GAJET where used as inputs for the calculation of the fictitious area using the Birch approach [22]. The H_2 jet was modeled as a circular source area whose diameter changed with time based on the calculations of the fictitious area by the Birch approach. Other conditions at the source were sonic velocity (1305 m/s), atmospheric pressure (101325 Pa) and temperature (313.15 or 293 K) for all scenarios. The differences in the release profiles, as shown in Figure 2 and Figure 3, between C1, C2 and C3 and between P1 and P2 scenarios

are attributed to the different leak diameters. For a given storage pressure, an increase in the leak diameter leads to an increased mass flow rate and a rapid release (C3 and P2 scenarios). For scenarios C1 and P1, the release was assumed constant until the H2 concentration at the sensor at the middle of the fan exceeds 20% of the LFL. An initial simulation with a release mass flow rate equal to the maximum of the profiles was set to find the arrival time of the 20% of the LFL at the sensor. The time was 5 seconds for C1 scenario whereas the P1 scenario the H2 concentration did not reach that value for 1000 seconds. Based on the UNIPI report [14] the H2 release was set constant for 15 seconds for scenario C1 (the extra 10 seconds were assumed to be the necessary time for the activation of the ESD (Emergency Shut Down) and the shut down of the system) and then the release had the profile of Figure 2. For scenario P1 and based on the initial simulation, the release was constant.

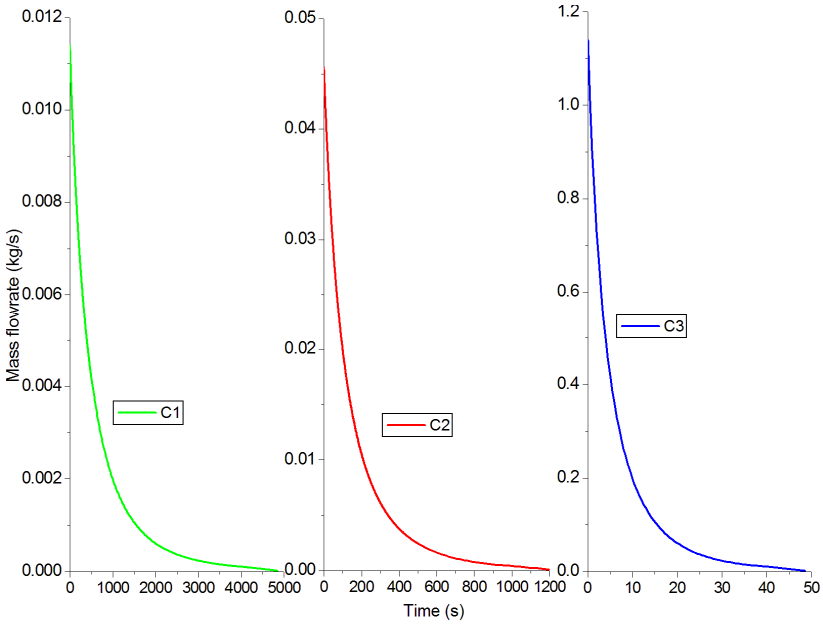

Figure 2: Calculated mass flow rates of C scenarios (GAJET code)

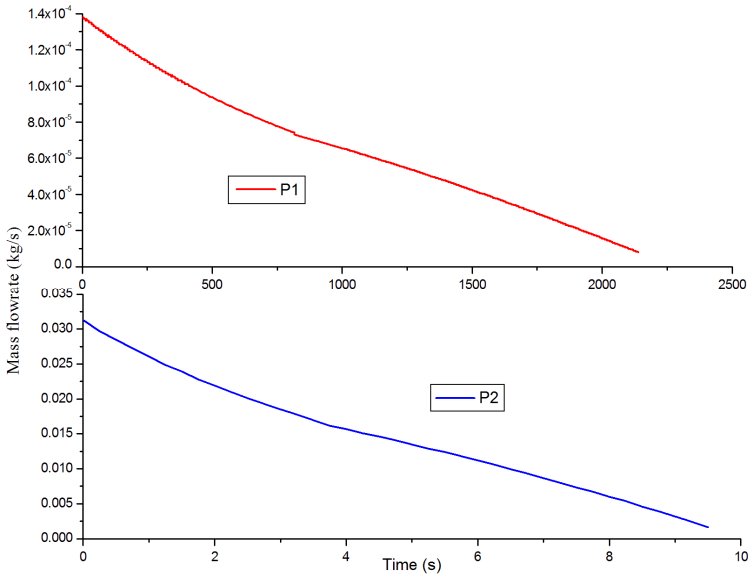

Figure 3: Calculated mass flow rates of P scenarios (GAJET code)

The dispersion calculations were performed in two steps. Each of the scenarios was initiated by activating only the fan. The simulations were set for 1000 seconds in order to ensure steady state conditions which were verified by the velocity profiles at several locations inside the buildings for each case. The release was then initiated based on the description of each scenario while the fan continued working. The mixing of H_2 with air was calculated by solving the three dimensional transient, fully compressible conservation equations for mixture mass (continuity equation), mixture momentum (for the three velocity components) and the H_2 vapor mass fraction transport equation.

The computational domain extended the boundaries of the buildings. The grid was Cartesian non-equidistant with its details given in Table 2. Grid independence check was not performed due to time limitations. The numerical options used were the first order implicit scheme for time integration and the first order upwind scheme for the discretization of the convective terms [23]. The increase of the time step was limited using a CFL=2.

Table 2: Grid characteristics of C1, C2, C3, P1 and P2 scenarios

Grid characteristics	C1	C2	C3	P1	P2
Minimum cell size (m)	0.1	0.1	0.1	0.04	0.1
Number o f cells in the X, Y and Z direction	31x53x28	31x52x28	31x51x28	35x55x31	27x43x27
Total number of cells	45.440	44.574	43.696	57.939	31.061

4.1.2 Results and discussion

Figure 4 shows the H2 mass and the mixture volume of the flammable cloud of scenarios C1, C2 and C3. The graphs show a maximum flammable volume (26 m^3, 58 m^3 and 57 m^3) at approximately 44, 34 and 7 seconds respectively. As the releases decreased with time, the flammable volume decreased to 1% of the enclosure volume at 780, 450 and 109 seconds whereas it reached the 0.1% of the enclosure volume at 1440, 750 and 222 seconds. Even though scenario C3 creates a high flammable volume, its residence time is the shortest. The differences in the residence times are attributed to the differences in the release flow rates and the release duration between the three cases (Figure 2). One possible risk reducing measure could be to increase the mechanical ventilation of the building or even considering locating the compression unit outdoors. Another measure could be to decrease the volume of the cooler at the minimum size needed based on the specifications of the fueling station, thus reducing the H2 amount to be released. Finally, gas detection at probe positions inside the building coupled to activation of emergency ventilation, relief of H2 to a safe area or purging, should be considered in order to detect the H2 leak soon and prevent further accumulation of H2 inside the building.

Figure 6 shows the H2 mass and the mixture volume of the flammable cloud of P1 and P2 scenarios. The flammable volume of P1 scenario was very limited ($1.68 \cdot 10^{-3} m^3$) whereas for P2 scenario its maximum value was 15.9 m^3 at 9 seconds. Again, the differences in the clouds are attributed to the different release flow rates and release durations. The volume of the flammable cloud of P2 scenario decreased to 1% of the enclosure volume at 31 seconds and to 0.1% of the enclosure volume at 58 seconds. The ventilation of the enclosure was sufficient for P1 scenario whereas for P2, the residence time of the flammable cloud was quite short. The residence time of the flammable cloud should be also taken into account for general safety considerations.

Criteria to assess the ventilation efficiency in enclosures and specifically for gas turbine enclosures are described in [24]. According to [24], the safety criteria define that (a) the 100% LEL equivalent stoichiometric volume (ESV) should be less than 0.1% of the net enclosure volume and (b) the 100% LEL equivalent stoichiometric volume should additionally be less than 1 m^3 in all cases, irrespective of the net enclosure volume.

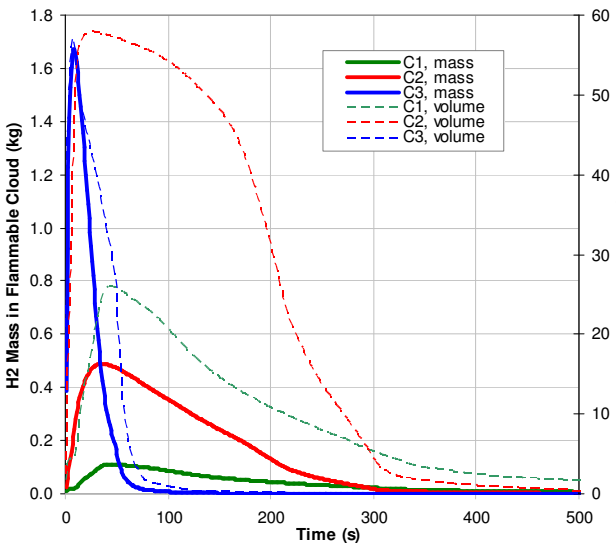

Figure 4: Compression building scenarios: H2 mass and volume of flammable cloud

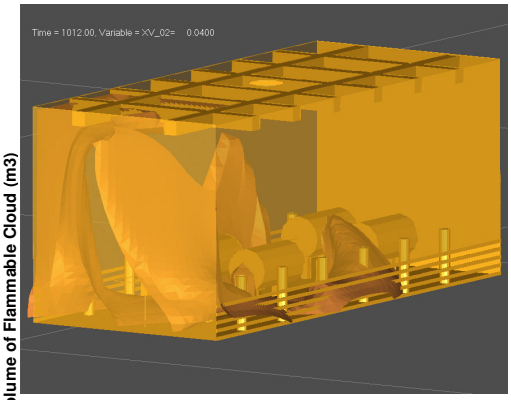

Figure 5: Compression building scenarios: LFL cloud at 12 seconds (C1 scenario)

	Max. Flamm. Volume	H2 mass
C1 scenario	26 m^3	0.112 kg
C2 scenario	57.7 m^3	0.487 kg
C3 scenario	57.1 m^3	1.65 kg

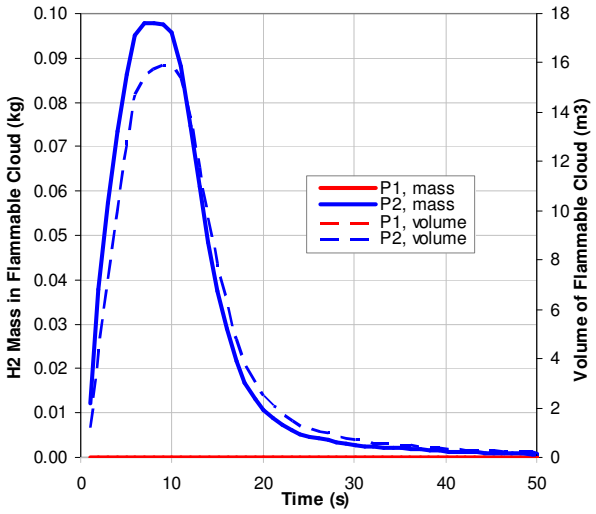

Figure 6: Purification building scenarios: H2 mass and volume of flammable cloud

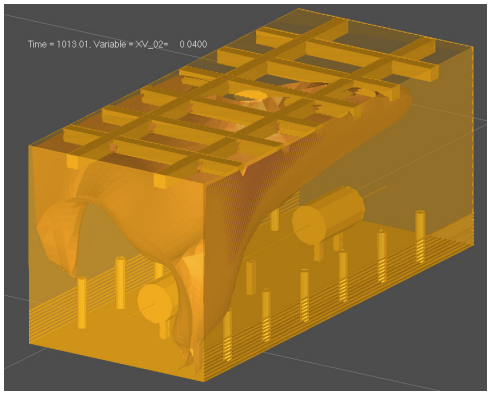

Figure 7: Purification building scenarios: LFL cloud at 13 seconds (P2 scenario)

	Max. Flamm. Volume	H2 mass
P1 scenario	$1.68 \cdot 10^{-3}$ m^3	$8.3 \cdot 10^{-6}$ kg
P2 scenario	15.9 m^3	$9.76 \cdot 10^{-2}$ kg

4.2 Open/semi-confined scenarios

Four scenarios concerning the storage cabinet were described by the UNIPI report. The first two scenarios (ST1 and ST2) were a small leak with two ambient wind velocities (1.5 and 5 m/s respectively). The other two scenarios (ST3 and ST4) were a rupture of a pipeline again with two wind velocities (1.5 and 5 m/s). The dimensions of the cabinet were 1m, 1m and 2m in X, Y and Z directions. The storage cabinet had vents at the bottom and top with 0.1m height. UNIPI described four scenarios concerning the storage bank. The first two (S1 and S2) were a large leak fed from the storage bank with 1.5 m/s and 5 m/s ambient wind velocity whereas the other two (S3 two S4) were a large leak from one cylinder with the same wind velocities. Finally, two scenarios concerning the dispensers (RF1 and RF2) covered a large leak from the refueling hose with two ambient wind velocities as above.

Table 3: Description of open/semi-confined scenarios

Scenario	Diameter of leak (m)	Leak direction	H2 inventory (m^3)	Temperature (K) and pressure (bar)	Prevailing wind velocity (m/s)
ST1	0.0008	downwards	0.1	293.15, 451	1.5
ST2	0.0008	downwards	0.1	293.15, 451	5
ST3	0.008	horizontal	0.1	293.15, 451	1.5
ST4	0.008	horizontal	0.1	293.15, 451	5
S1	0.0016	downwards	12.5	293.15, 451	1.5
S2	0.0016	downwards	12.5	293.15, 451	5
S3	0.0016	downwards	2.5	293.15, 451	1.5
S4	0.0016	downwards	2.5	293.15, 451	5
RF1	0.0016	downwards	0.15	293.15, 451	1.5
RF2	0.0016	downwards	0.15	293.15, 451	5

4.2.1 Release and dispersion calculations

The release calculations were done with the integral code GAJET. For ST1 and ST2 scenarios, the amount of H2 released was much smaller than the maximum expected flow in the pipeline, therefore a constant release for the time necessary to refill a car was assumed (70 seconds). After that, the pressure drop inside the filter was assumed enough to be detected thus the release was decreasing causing the emptying of the filter. For ST3 and ST4 scenarios the pressure drop due to the rupture was assumed to activate the ESD after 5 seconds. Thus, a constant release of 5 seconds was followed by a decreasing release. For RF1/RF2 scenarios it was assumed that the operator needs 1 minute to activate the ESD system and that the line closes in 5 seconds after the activation. Thus, the release was constant for 65 seconds and then decreased due to the emptying of the inventory. The results from GAJET where taken as inputs for the calculation of the fictitious area using the Birch approach. The conditions at the source were sonic velocity (1305 m/s), atmospheric pressure (101325 Pa) and temperature (293 K) for all scenarios. The differences in the release profiles between ST1/ST2 and ST3/ST4 are attributed to the different leak diameters. For a given storage pressure, an increase in the leak diameter leads to an increased mass flow rate and a rapid release (ST3/ST4 scenarios). The differences in the release profiles between S1/S2, S3/S4 and RF1/RF2 are attributed to the different released H2 inventory.

The dispersion calculations consisted of three stages. In the first stage, the steady state 1D vertical profile of the wind velocity and turbulence was calculated. In the second stage, the 3D flow field over the BBC station and its surroundings was calculated using the previously obtained profiles spread over the 3D domain as initial conditions. The domain covered the BBC station and its surroundings to capture the effects of all buildings to the velocity field.

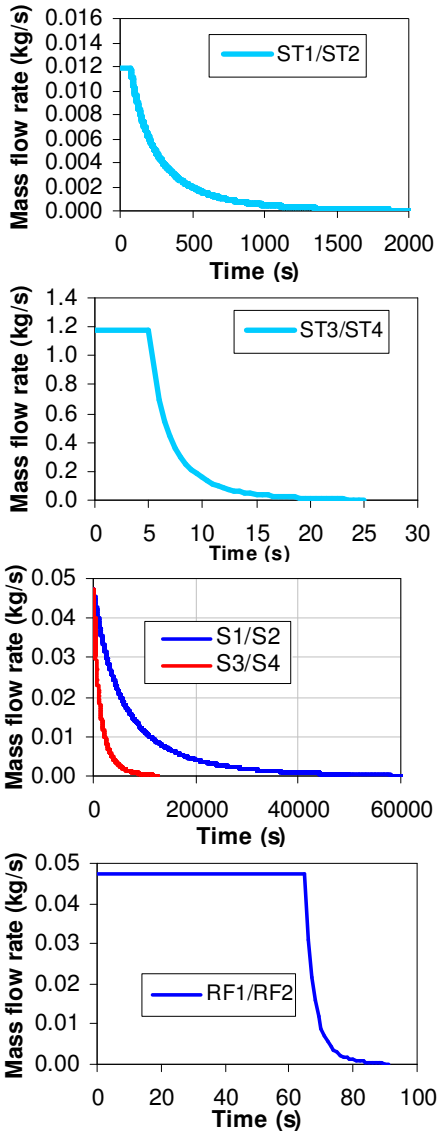

Figure 8: Calculated release flow rates

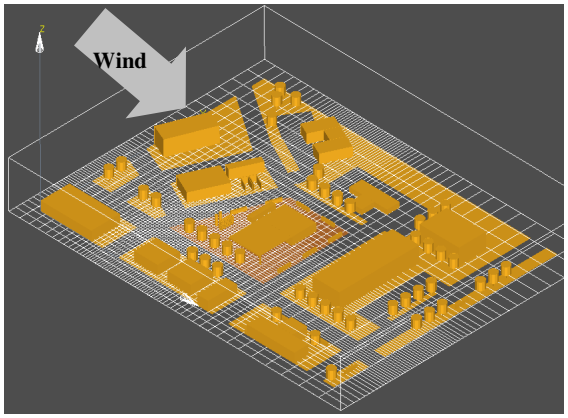

Figure 9: 3d Steady State computational domain

The domain and the direction of the wind used in all scenarios are shown in Figure 9. Finally, the H_2 dispersion was calculated using the previously obtained three dimensional steady state field as initial conditions. This time the domain covered only the part of the BBC station that was assumed to contain the dispersed H2 for each scenario thus saving computational time. The same numerical options as in the previous scenarios were used.

Table 4: Grid characteristics of 3D Steady State, (ST), (S) and (RF) scenarios

Scenario	Minimum cell size in X, Y and Z (in m)	Cells in X, Y and Z	Total number of cells
3D Steady State	1.48 in X, Y and 0.2 in Z	62x57x26	87.900
ST1/ST2 dispersion	0.2	54x49x32	83.989
ST3/ST4 dispersion	0.2	54x48x32	82.418
S1/S2 dispersion	0.2	53x45x34	80.335
S3/S4 dispersion	0.2	52x45x34	78.733
RF1/RF2 dispersion	0.2	56x46x31	78.876

4.2.2 Results and discussion

Figure 10 and Figure 11 show the H2 mass and the mixture volume of the flammable cloud of ST1/ST2 and ST3/ST4 scenarios. The increase of the wind velocity did not significantly influence the clouds. The ST1/ST2 flammable clouds decreased to zero after almost 1300 seconds. The maximum values of the ST3/ST4 clouds are higher than the ones of ST1/ST2 scenarios whereas the clouds disappeared at approximately 30 seconds. The differences are attributed to the differences in the release flow rates and the release duration between the cases. The difference between the clouds of ST3 and ST4 are again not significant. Figure 12 and Figure 13 show the H2 mass and the mixture volume of the flammable cloud of S1, S2, S3 and S4 scenarios. The maximum values of the clouds are not significantly different. This is attributed to the same initial release flow rate. The residence time of the flammable clouds of S1 and S2 are quite close. The same holds for S3 and S4 scenarios. Again, the increase of the wind velocity did not affect considerably the flammable clouds. UNIPI also made dispersion calculations for these scenarios. For S1 and S3 scenarios UNIPI's maximum flammable cloud increased by 130-200% whereas for S2 and S4 decreased by 93-95%. By comparing the input data it was found that there were some differences in the initial H2 inventories and thus in the H2 released mass. Nonetheless, it seems that Effects model is very sensitive to wind conditions especially because it is not able to take into account the effects of buildings and the arrangement of the systems involved (piping, storage vessels, etc.). Figure 14 shows the H2 mass and the mixture volume of the flammable cloud for RF1/RF2 scenarios. The peak is reached at 20 and 13 seconds respectively. The values of H2 mass and cloud volume are not influenced significantly by the increase of the wind. On the contrary, UNIPI's maximum flammable mass increased by 150% for RF1 and decreased by 90% for RF2 scenario.

In order to examine the influence of the wind further, the ratio of the size of the flammable cloud in the x, y and z direction with wind velocity 5 m/s to the ones with wind velocity 1.5 m/s of the NCSRD results, are shown in Figure 15. Generally, there is a decrease in the size of the flammable clouds but the decrease didn't exceed by a factor of 2. This can be attributed to the fact that the steady state 1D

vertical profile of the wind velocity and turbulence was set outside the BBC station creating a 3D flow field that covered not only the station but also its surrounding buildings. The velocity field within the area of the filling station was lower than the predefined value of 5 m/s.

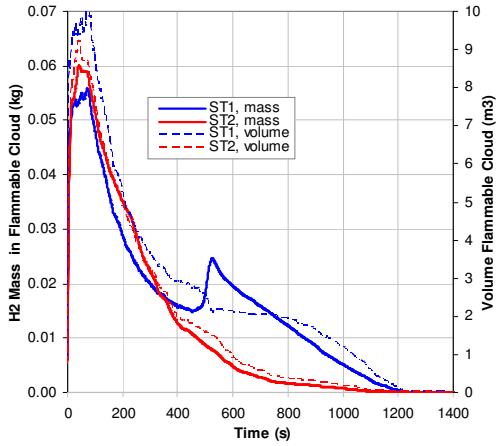

Figure 10: H2 mass and volume of flamm. cloud

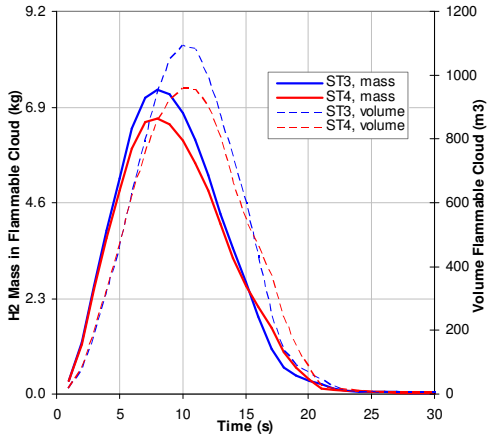

Figure 11: H2 mass and volume of flammable cloud

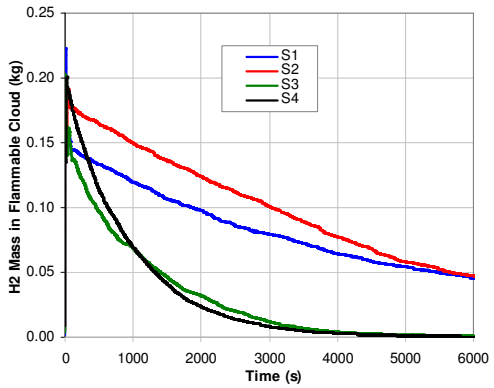

Figure 12: H2 mass in flammable cloud

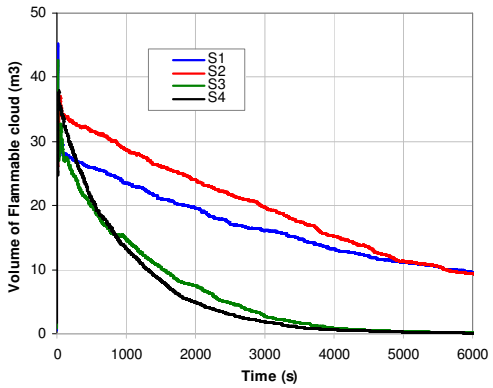

Figure 13: Volume of flammable cloud

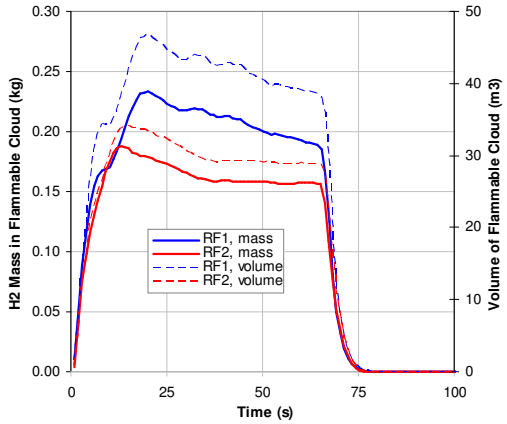

Figure 14: H2 mass and volume of flamm. cloud

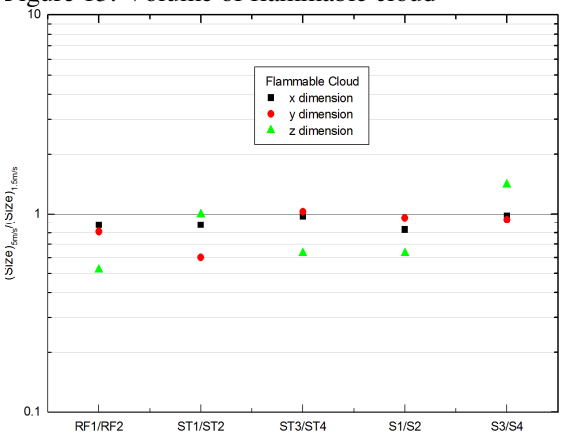

Figure 15: Effect of wind on size of flammable cloud

5 CONCLUSIONS

A quantitative analysis performed by NCSRD within the internal project HyQRA of the HYSAFE NoE co-funded by EC, is presented. Partners NCSRD and UNIPI collaborated on a common QRA of a predefined hypothetical gaseous hydrogen fueling station. UNIPI identified the hazards on site, selected the most critical ones, defined the events that could be the primary cause of an accident and

provided to NCSRD the scenarios listed in risk order. NCSRD performed the quantitative analysis using the integral code GAJET and the ADREA-HF CFD code. Five scenarios covered hydrogen releases in ventilated buildings (compression and purification buildings). The remaining scenarios were releases in open/semi-confined environment (storage cabinet, storage bank and dispensers). The predicted spatial and transient evolution of the formed flammable hydrogen-air clouds in the realistic geometry were provided to UNIPI for analysis of the consequences and evaluation of the risk and distances of damage to suggest improvements in the design and management of the BBC station to reduce the risk.

Concerning the scenarios of the compression building, it was found that the worst scenario was the one with the largest leak diameter. Differences in the residence time and peaks of the clouds between the three scenarios were found due to the different release profiles. Suggestions to decrease the flammable volume and its residence time cover the following: (a) increase of the mechanical ventilation inside the building or even considering placing the compression unit outdoors, (b) decrease of the volume of the cooler at the minimum size needed (c) use of gas detection at probe positions inside the building coupled to activation of emergency ventilation, relief of H2 to a safe area or purging.

The scenario with the smallest leak inside the purification building created an insignificant flammable volume whereas for the scenario with the largest leak diameter in the same building, the residence time of the flammable cloud was quite short.

Not only the existence of a flammable cloud, but also its residence time should be taken into account for general safety considerations.

The simulations of the open/semi-confined scenarios showed that the increase in the wind velocity affects the size of the flammable clouds but not significantly. The limited effect of the higher wind velocity is attributed to the presence of the surrounding buildings causing a wind velocity field within the fueling station much lower than the initially defined wind velocity.

6 ACKNOWLEDGMENTS

The authors would like to thank the European Commission for co-funding of this work in the framework of the HySafe FP6 Network of Excellence (contract no. SES6-CT-2004-502630).

7 REFERENCES

[1] Fuel cells 2000, “Worldwide Hydrogen Fuelling Stations”, updated 10/08, www.fuelcells.org

[2] LaChance, J., Tchouvelev. A., Ohi, J., “Risk-informed process and tools for permitting hydrogen fueling stations”, 2nd International Conference on Hydrogen Safety, San Sebastian, Spain, 11-13 Sept., 2007

[3] Chitose, K., Ogushi, H., Kawai, K., Mizuno, Y. and Sadanori, A., “Risk Assessment Methodology for Hydrogen Refueling Station”, WHEC 16, Lyon France, 13-16 June, 2006

[4] Nilsen, S., Marangon, A., Middha, P., Engeboe, A., Markert, F., Ezponda E. and Chaineaux, J., “Determination of hazardous zones for a generic hydrogen station – a case study”, 2nd International Conference on Hydrogen Safety, San Sebastian, Spain, 11-13 Sept., 2007

[5] Haugom, G. P., Holmefjord, K. O. and Skogseth, L. O., “Assessment and evaluation of 3rd party risk for planned hydrogen demonstration facility”, 2nd International Conference on Hydrogen Safety, San Sebastian, Spain, 11-13 Sept., 2007

[6] LaChance, J. L., “Risk-informed separation distances for hydrogen refuelling station” , 2nd International Conference on Hydrogen Safety, San Sebastian, Spain, 11-13 Sept., 2007

[7] Kikukawa, S., Mitsuhashi, H. and Miyake A., "Risk assessment for liquid hydrogen fueling stations", International Journal of Hydrogen Energy, 34, 2009, pp. 1135-1141

[8] Middha, P. and Hansen O.R., "Using computational fluid dynamics as a tool for hydrogen safety studies", Journal of Loss Prevention in the Process Industries, 2008, in press, doi:10.1016/j.jlp.2008.10.006

[9] A.G. Venetsanos, E. Papanikolaou, J.G. Bartzis, The ADREA-HF CFD code for consequence assessment of hydrogen applications, 3rd International Conference on Hydrogen Safety, Ajaccio, Corsica, France, 16-18 September, 2009

[10] HySAFE, Safety of hydrogen as an energy carrier, Network of Excellence, FP6, Available from: www.hysafe.org, 2003-2009

[11] TNO Safety Software, EFFECTS DAMAGE, Version 7, TNO Built Environment and Geosciences, Department of Industrial and External Safety, www.tno.nl/effects

[12] Olav Hansen, Prankul Middha, Alessia Marangon, Marco Carcassi, Koos Ham, Nico Versloot, "Description of a Gaseous Hydrogen Refueling Station – Benchmark Base Case (BBC) for HyQRA IP 3.2", Feb 2008

[13] Communication with Prankul Mddha, GEXCON, via e-mail in June 08, Comments on BBC geometry sent from UNIPI via e-mail in June 08, Communication with Prankul Mddha, GEXCON, via e-mail in July 08

[14] Schiavetti M., Marangon A., Carcassi M., "Scenario selection: C-building, Storage Cabinet, Storage bank, Dispensers, P-building", 5/08/08

[15] Venetsanos, A. G, Huld, T., Adams, P., Bartzis, J. G., 2003, "Source, Dispersion and Combustion Modelling of an Accidental Release of Hydrogen in an Urban Environment", *Journal of Hazardous Materials*, A105, pp. 1-25

[16] Bartzis J.G., "ADREA-HF: A three-dimensional finite volume code for vapour cloud dispersion in complex terrain", EUR Report 13580 EN

[17] Papanikolaou E.A. and Venetsanos A.G., CFD simulations of hydrogen release and dispersion inside the storage room of a hydrogen refuelling station using the ADREA-HF code, 2nd International Conference on Hydrogen Safety, San Sebastian Spain, September, 2007

[18] Launder B.E. and Spalding D.B., "The numerical computation of turbulent flow", Computer Methods in Applied Mechanics and Engineering, 3, Issue 2, pp. 269-289

[19] N.C. Markatos, "Mathematical Modelling of Turbulent Flows", Appl. Math. Modelling, Vol. 10, 3, pp. 190-220, 1986

[20] N.C. Markatos, M.R. Malin, G. Cox, "Mathematical Modelling of Buoyancy-Induced Smoke Flow in Enclosures", Int. J. Heat Mass Transfer, Vol. 25, No. 1, pp. 63-75, 1982 AND Correspondence, Int. J. Heat Mass Transfer, Vol. 25, No. 11, pp. 1777-1778, 1982

[21] N.C. Markatos, K.A. Pericleous, "Laminar and turbulent natural convection in an enclosed cavity", Int. J. Heat Mass Transfer, Vol. 27, 5, pp. 755-772, 1984

[22] Birch, A.D., Brown, D.R., Dodson, M.G., and Swaffield, F., 1983, "The Structure and Concentration Decay of high Pressure Jets of Natural Gas",Combustion Science and Technology 36: 249-261

[23] Patankar S.V., 1980, "Numerical heat transfer and fluid flow", Hemisphere Corporation

[24] Ivings, M., Lea, C., Ledin, H.S., Pritchard, D., Santon, R. and Saunders J., "Outstanding safety questions concerning the use of gas turbines for power generation", HSL Summary Report, CM/04/09